



### On the spectral numerical study of magneto – convective flow of Jeffery fluid through Poro-elastic media with thermal radiation and buoyancy effects

Lead Author

**OSHO, Femi Timothy**

Affiliation:

Department of Mathematics, Adeyemi Federal Univeristy of Education, Ondo, Ondo State, Nigeria



#### **Abstract**

Many physiological systems involving soft tissues depend on flow through a deformable porous media; coronary blood, for example, flows through arteries containing arteriosclerosis. Systems that permit highly viscous pressure force flows through elastic porous materials are said to be deformable. A novel mathematical model for the nonlinear convective flow for large temperature differences is developed based on this supposition. The constant magneto-convective flow of Jeffery fluid through a deformable porous material with nonlinear convection and heat radiation is the subject of this inquiry. The solid displacement, flow velocity, and energy equations' governing equations are built using well-established flow assumptions and one-way flow inside the impermeable vertical walls. The governing equations' dimensionless form is solved using the Spectral Chebyshev Collocation methods, and the fourth-order Shooting-Runge-Kutta Scheme is used to validate the solution. The Spectral Quasilinearization method is utilized in the limiting situation and validated against the body of existing research. The impacts of each flow parameter are explained through the display of graphic data. Tabular representation is also provided for results convergence and comparison. Understanding heat transport to soft tissues, particularly during hyperthermia for cancer treatment, is important, and this study contributes to that understanding.

**Keywords:** magneto-convective flow, poro-elastic media, thermal radiation, buoyancy effects



**Co-Author: Adesanya Samuel O.** Department of Mathematics and Statistics, Redeemer's University Ede, Osun State, Nigeria.

## 1.0 Introduction

Magneto-convection in porous media has garnered significant attention due to its applications in geothermal reservoirs, heat exchangers, and electromagnetic devices. Studies on magneto-convection date back to the 1960s Chandrasekhar, S. (1961). Recent research focuses on magnetic fluid effects on convective flows [Finlayson (1972), Kaloni and Lou (2000), Siddiqa and Hossain (2013), Sheikholeslami and Ganji (2015)]. For example, Bhattacharyya et al. (2019) analyzed magnetohydrodynamic flow in a porous medium. Numerous studies have revealed explored minimizing entropy formation in biological magneto-thermal fluid dynamics from computing entropy production rates and Bejan numbers in magnetized biofluid transfer (Beg *et al.*, 2013) to analyzing entropy formation in magnetohydrodynamic viscoelastic nanofluid bio convection in a Darcian porous regime in thin film reactive mixed convection (Khan *et al.*, 2019). Studies have looked at the effects of thermal radiation on entropy formation in dual immiscible non-Newtonian Stokes' pair stress fluids, such as heat transfer and channel flow (Ramana Murthy et al., 2017), as well as how it contributes to the formation of entropy in non-Newtonian power-law convection from an axisymmetric stretched sheet through coupled radiative and viscous dissipation effects (Jamalabadi et al., 2016).

The investigation into the flow of fluids within non-deformable permeable media stands as a dynamic field of research, embracing diverse branches of engineering and science. Numerous natural and industrial processes involve flexible mediums, such as insulation, Bio-materials, and geo-materials, where the forces in fluid flow can cause significant deformations. The resulting impact on fluid flow becomes pronounced when with deformation, the characteristics of the material controlling fluid flow alter. Deformable porous media necessitate a concurrent solution for the equations for viscous flow and elastic deformation, a challenge addressed by the theory of mixtures elucidated by Biot (1941) within the geo-mechanics context. Zhao *et al* (2023) studied the transportation behavior of a porous media using a sandback model. Bui and Nguyen (2017) utilized the coupled approach of solid and fluid in a deformable porous medium, Rohan *et al* (2019) considered the flow in a deformable double-porous structure described at two characteristic scales. Poro-elasticity theory, introduced by Biot (1956), describes fluid-solid interactions in porous materials. Studies have explored poro-elastic media's

---

influence on fluid flow [Bear (1972), Bowen (1980), Coussy (1995)]. Ouyang et al. (2020) investigated flow through porous media with elastic deformation.

Research on non-Newtonian fluids, particularly Jeffery fluid, has grown due to its applications in biological and engineering systems [Tanner (1968), Sochi (2010), Fang (2013)]. Jeffery fluid's viscoelastic properties are crucial in modeling blood flow and polymer solutions. Studies, such as those by Adesanya et al. (2017) on third-grade Reiner-Rivlin fluids with chemical reactions and Kumar et al. (2019) have explored entropy production and heat line visualization analysis on time-dependent free convection flow of a second-grade elastic-viscous fluid. The Jeffrey fluid model, a versatile nonlinear viscoelastic hydrodynamic model, has been widely used to represent biophysical fluids, with studies by Varjaveluet al. (2011) highlighting its applicability. Mathematical studies, such as those by Manzoor et al. (2018) employing the method of Adomian decomposition, have investigated propulsion of Jeffrey's viscoelastic fluids in porous media by hydromagnetic ciliated media channels, observing significant modifications in momentum as well as thermal properties. Ramesh et al. (2018) theoretically examined the peristaltic pumping of viscoelastic two-phase blood using magnetohydrodynamics (MHD), noting the impact of Jeffrey's viscoelastic parameter on fluid and particle phase flow, axial pressure gradient, and pressure differential in the area of pumping.

Thermal radiation plays a vital role in energy transfer, especially in high-temperature applications. Researchers have incorporated radiation effects into convective flow models [Siegel and Howell (1972), Viskanta (1996), Takhar (1998)]. For instance, Makinde et al. (2007) examined radiation effects on MHD flow. Applications for research on viscous fluid flow with thermal radiation can be found in heating and cooling processes, as well as in space technology and high-temperature processes for effective system performance. Medical equipment is sterilized using thermal radiation, cancer and tumor treatment in hospitals, and in bakeries, toasting bread, cakes, and meat pies. Technological engineering incorporates this idea in the production of boilers, heaters, air conditioners, and processing crude oil. Rosseland (1931) initially provided the expression for radiation, subsequently made simpler by Cess and Sparrow (1962), and subsequently utilized in studies by Makinde et al. (2007), Makinde and Ibrahim (2011), Ganji et al. (2012), Sheikholesmi (2015), and Abel and Mashasha (2007). Some scholars discuss the impact of heat radiation using linearized radiative heat flux, while others, such as Magyari and Pantokratoras (2011), argue for a more realistic



approach using non-linear radiative heat flux. Novelty-related studies on this approach could be found in Mansour (1990), and Jha *et al.* (1990).

Despite existing research, a comprehensive spectral numerical study integrating magneto-convection, Jeffrey fluid, poro-elastic media, thermal radiation, and buoyancy effects remains unaddressed. Numerous scholars have investigated fluid dynamics, considering flow through permeable conduits because of its importance in drainage, electronic materials' cooling/heating, and thermal insulation. Porosity enhances fluid suction/injection through pore spaces, illustrated in computer engineering cabinets intended to be channel-shaped for both human survival and cooling use of pores for breathing in air and perspiring. Ajibade *et al.* (2011), Miyatake *et al.* (1976), and Al-Nimr and Haddad (1999) examined convection flows in nature under varying pathway wall situations.

## 2. Influence of Nonlinear Thermal Radiation and Buoyancy on Magneto-Convective Flow of Jeffery Fluid through a Deformable Porous Medium

$$\mu \frac{d^2U}{dY^2} - (1-\phi) \frac{dP}{dX} + KV = 0 \quad (1)$$

$$\frac{2\mu_a}{1+\lambda_1} \frac{d^2V}{dY^2} - \phi \frac{dP}{dX} - KV - \sigma B_0^2 V + \rho g \beta_0 (T - T_0) + \rho g \beta_1 (T - T_0)^2 = 0 \quad (2)$$

$$\frac{K_0}{\rho c_\rho} \frac{d^2T}{dY^2} + \frac{2\mu_a}{(1+\lambda_1)\rho c_\rho} \left( \frac{dV}{dY} \right)^2 + \frac{4\sigma^*}{\rho c_\rho 3k^*} \frac{d^2T^4}{dY^2} + \frac{(K + \sigma B_0^2)V^2}{\rho c_\rho} = 0 \quad (3)$$

Given the boundary conditions to be:

$$\frac{dU}{dY} = 0, \frac{dV}{dY} = 0, \frac{d\theta}{dY} = 0, \text{ at } Y = 0, \quad (4)$$

Presenting the dimensionless variables and parameters

Putting the dimensionless variables of equation (5) in (1) to (4) to have

$$\left. \begin{aligned} y &= \frac{Y}{h}, x = \frac{X}{h}, v = \frac{2\mu_a V}{\rho g \beta h^2 (T_1 - T_0)}, u = \frac{\mu U}{\rho g \beta h^2 (T_1 - T_0)}, \\ \theta &= \frac{T - T_0}{T_1 - T_0}, p = \frac{P}{\rho g \beta h (T_1 - T_0)}, \kappa = \frac{\rho^2 g^2 \beta^2 h^2 (T_1 - T_0)}{2\mu_a K_0} \\ \delta &= \frac{Kh^2}{2\mu_a}, M = B_0 h \sqrt{\frac{\sigma}{2\mu_a}}, \alpha = \frac{(Q_0 h^2)}{K_0}, \end{aligned} \right\}$$

(5)

$$\left. \begin{aligned} \frac{d^2 u}{dy^2} - (1 - \phi) \frac{dp}{dx} + \delta v &= 0 \\ \frac{1}{1 + \lambda_1} \frac{d^2 v}{dy^2} - \phi \frac{dp}{dx} - \delta v - M^2 v + \theta(1 + \gamma \theta) &= 0 \\ \frac{d^2 \theta}{dy^2} + \frac{\kappa}{(1 + \lambda_1)} \left( \frac{dv}{dy} \right)^2 + (\delta + M) \kappa v^2 + R \left[ 4(\theta + \phi)^2 \theta'^2 + \frac{4}{3}(\theta + \phi)^3 \theta'' \right] &= 0 \end{aligned} \right\}$$

(6)

The suitable boundary conditions are:

$$u = 0, v = 0, \theta = 1 \text{ at } y = 1$$

(7)

### Weighted Residual Method of Solution

By assuming an admissible solution of the Chebyshev polynomials form

$\Phi_j(y)$  as a sum of  $N+1$  in which

$$\begin{aligned} u(y) &\approx u^N(y) = \sum_{j=0}^N a_j \Phi_j(y), \\ \theta(y) &\approx \theta^N(y) = \sum_{j=0}^N b_j \Phi_j(y), \\ \phi(y) &\approx \phi^N(y) = \sum_{j=0}^N c_j \Phi_j(y) \end{aligned}$$

(8)



Where the  $(a_j, b_j, c_j)$  are coefficients to be determined based on the specified boundary conditions in (3.3.8)

$$\left. \begin{aligned} R_1 &= u_{yy}^N - (1-\phi) \frac{dp}{dx} + \delta v_y^N \\ R_2 &= \frac{1}{1+\lambda_1} v_{yy}^N - \phi \frac{dp}{dx} - \delta v^N - M^2 v^N + \theta^N (1+\gamma \theta^N) \\ R_3 &= \theta_{yy}^N + \frac{\kappa}{(1+\lambda_1)} v_y^{2N} + (\delta+M) \kappa v^{2N} + R \left[ 4(\theta^N + \phi)^2 \theta_y^{2N} + \frac{4}{3} (\theta^N + \phi)^3 \theta_{yy}^N \right] \end{aligned} \right\} \quad (9)$$

together with

$$u^N(\pm 1) = 0, \theta^N(\pm 1) = \theta_w, \phi^N(\pm 1) = 1. \quad (10)$$

The residues are forced to zero at the Gauss-Lobato points to get a system of nonlinear algebraic equations at

$$R_1(y_j) = R_2(y_j) = R_3(y_j) = 0, \quad j = 0, 1, 2, \dots, N \quad (11)$$

where  $y_j$  are defined

$$y_j = \frac{1}{2} \left( 1 - \cos \left( \frac{j\pi}{N} \right) \right), \quad j = 0, 1, 2, \dots, N \quad (12)$$

The result of numerical computation of (8) - (12) is presented in section four in both graphical and tabular form. Next, the Shooting Runge-Kutta of order four is used to validate the spectral Chebyshev Collocation method. Both Graphical and tabular are presented below.

Validation by Shooting RK-4 code.

### 3. Graphical and Tabular Results for the Influence of Nonlinear Thermal Radiation and Buoyancy on Magneto-Convective Flow of Jeffery Fluid Through a Deformable Porous Medium

**Table 3.1:** Validation of Numerical Result when  $N_y=30; \delta=1; M=0.1; \phi=0.6; G=-1; \lambda_1=0.2; R=0.1; m=0.1; \xi=0.1; \gamma=0.1;$

| Y     | u(y)-Shooting-RK4                  | u(y)-SCM                             | ABSOLUTE ERROR                      |
|-------|------------------------------------|--------------------------------------|-------------------------------------|
| -1    | 0.                                 | $-2.00550371815531 \times 10^{-17}$  | $2.00550371815531 \times 10^{-17}$  |
| -0.75 | 0.20031250311834384                | 0.20031249919329736                  | $3.925046482278205 \times 10^{-9}$  |
| -0.5  | 0.3564374323907538                 | 0.3564374280700931                   | $4.32066071809345 \times 10^{-9}$   |
| -0.25 | 0.4551461632826773                 | 0.4551461623522259                   | $9.304514381192064 \times 10^{-10}$ |
| 0.0   | 0.488869989403844                  | 0.48886998921520053                  | $1.886434897180322 \times 10^{-10}$ |
| 0.25  | 0.45514616272811137                | 0.4551461623522259                   | $3.758854894009289 \times 10^{-10}$ |
| 0.5   | 0.3564374285811989                 | 0.3564374280700931                   | $5.111058243301159 \times 10^{-10}$ |
| 0.75  | 0.20031250045577953                | 0.20031249919329736                  | $1.26248217435787 \times 10^{-9}$   |
| 1     | $1.253974548218617 \times 10^{-8}$ | $-1.917126492377182 \times 10^{-11}$ | $1.253974567389882 \times 10^{-9}$  |

**Table 3.2:** Validation of Numerical Result when  $N_y=30; \delta=1; M=0.1; \phi=0.6; G=-1; \lambda_1=0.2; R=0.1; m=0.1; \xi=0.1; \gamma=0.1;$

| Y     | v(y)-Shooting-RK4                   | v(y)-SCM                            | ABSOLUTE ERROR                      |
|-------|-------------------------------------|-------------------------------------|-------------------------------------|
| -1    | $-1.35525271560688 \times 10^{-20}$ | $3.757615583962017 \times 10^{-17}$ | $3.758970836677624 \times 10^{-17}$ |
| -0.75 | 0.3157506487084785                  | 0.31575066684751807                 | $1.813903954817064 \times 10^{-8}$  |
| -0.5  | 0.5261333101038975                  | 0.5261333259722585                  | $1.58683609585708 \times 10^{-8}$   |
| -0.25 | 0.6465007793418491                  | 0.6465007895729714                  | $1.023112228271116 \times 10^{-8}$  |
| 0.0   | 0.6856663266329883                  | 0.685666330282717                   | $6.395283413951347 \times 10^{-9}$  |
| 0.25  | 0.6465007863840315                  | 0.6465007895729714                  | $3.188939889930964 \times 10^{-9}$  |
| 0.5   | 0.5261333261439017                  | 0.5261333259722585                  | $1.716432551646107 \times 10^{-10}$ |
| 0.75  | 0.31575067137670887                 | 0.31575066684751807                 | $4.529190800184324 \times 10^{-9}$  |
| 1     | $1.028098524203779 \times 10^{-8}$  | $3.828112124543713 \times 10^{-17}$ | $1.028098520375667 \times 10^{-8}$  |

**Table 3.3:** Validation of Numerical Result when  $N_y=30; \delta=1; M=0.1; \phi=0.6; G=-1; \lambda_1=0.2; R=0.1; m=0.1; \xi=0.1; \gamma=0.1;$

| Y     | θ(y)-Shooting-RK4  | θ(y)-SCM           | ABSOLUTE ERROR                      |
|-------|--------------------|--------------------|-------------------------------------|
| -1    | 1.                 | 0.9999999999999999 | $1.110223024625156 \times 10^{-16}$ |
| -0.75 | 1.0129181837958283 | 1.012918189217893  | $5.422064575100194 \times 10^{-9}$  |
| -0.5  | 1.0202884258916065 | 1.02028843531813   | $9.426523561728573 \times 10^{-9}$  |
| -0.25 | 1.02421316786971   | 1.0242131693364636 | $1.466753607459736 \times 10^{-9}$  |
| 0.0   | 1.0254605914412989 | 1.0254605916729322 | $2.316333791441138 \times 10^{-10}$ |
| 0.25  | 1.0242131670520584 | 1.0242131693364636 | $2.284405109520548 \times 10^{-9}$  |
| 0.5   | 1.020288432707834  | 1.02028843531813   | $2.610295979366128 \times 10^{-9}$  |
| 0.75  | 1.0129181781170307 | 1.012918189217893, | $1.110086222944062 \times 10^{-8}$  |
| 1     | 0.9999999755546277 | 0.9999999999999999 | $2.444537217094478 \times 10^{-8}$  |

**Table 3.4: Convergence of SCCM when  $N_p=60; \delta=1; M=0.1; \kappa=0.6; G=-1; \lambda_1=0.2; R=0.1; m=0.1; \xi=0.1; \gamma=0.1;$**

| $N_p$ | U                   | V                  | $\theta$           |
|-------|---------------------|--------------------|--------------------|
| 5     | 0.356303311981987   | 0.5263031553951469 | 1.0205020494816825 |
| 10    | 0.3564374281991103  | 0.5261333260226033 | 1.020288438036291  |
| 15    | 0.3564374280700968  | 0.5261333259722658 | 1.0202884353182002 |
| 20    | 0.35643742807009315 | 0.5261333259722586 | 1.0202884353181303 |
| 25    | 0.35643742807009315 | 0.5261333259722586 | 1.0202884353181303 |
| 30    | 0.3564374280700931  | 0.5261333259722585 | 1.02028843531813   |
| 35    | 0.3564374280700931  | 0.5261333259722585 | 1.0202884353181303 |
| 40    | 0.3564374280700931  | 0.5261333259722585 | 1.0202884353181303 |

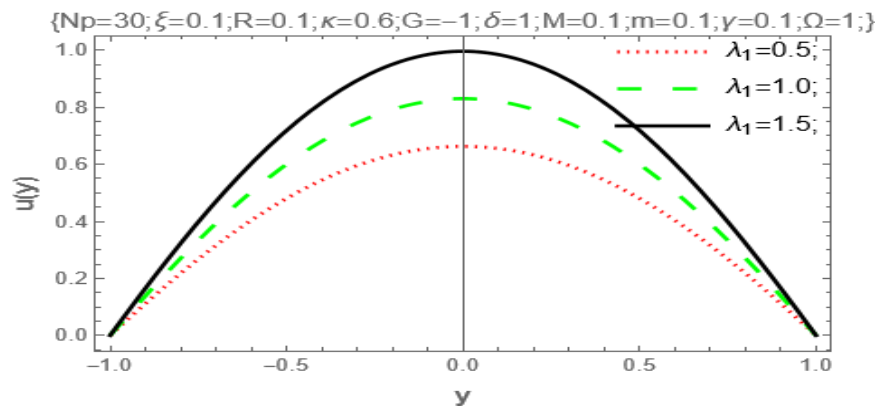


**Figure 3.1: Effect of Jeffrey parameter on solid displacement**  
 { $N_p=30; \xi=0.1; R=0.1; \kappa=0.6; G=-1; \delta=1; M=0.1; m=0.1; \gamma=0.1; \Omega=1;$ }

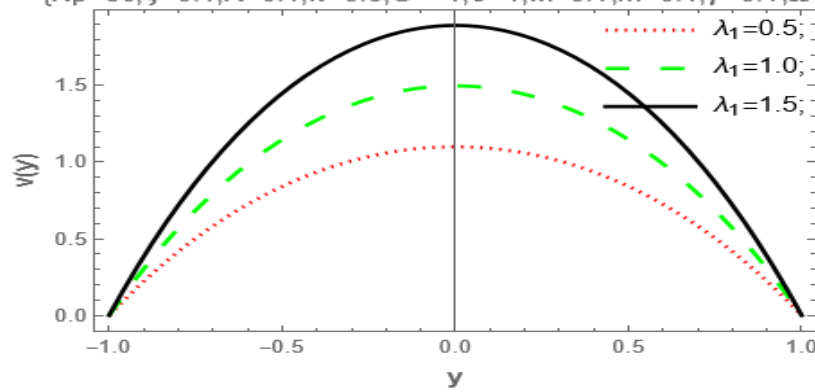


**Figure 3.2:** Effect of Jeffrey parameter on flow velocity  
 $\{Np=30; \xi=0.1; R=0.1; \kappa=0.6; G=-1; \delta=1; M=0.1; m=0.1; \gamma=0.1; \Omega=1;\}$

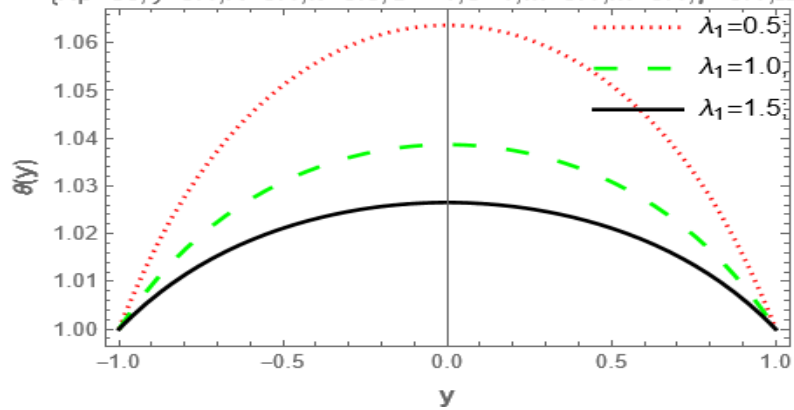


**Figure 3.3:** Effect of Jeffrey parameter on fluid temperature  
 The effect of Jeffrey parameter on the solid displacement, flow velocity and fluid temperature as shown in figures (3.1) –(3.3). The result shows that as Jeffrey parameter increases solid displacement and flow velocity rises while temperature decreases.

$\{Np=30; \xi=0.1; m=0.1; \kappa=0.6; G=-1; M=0.1; R=0.1; \lambda_1=0.1; \gamma=0.1; \Omega=1;\}$

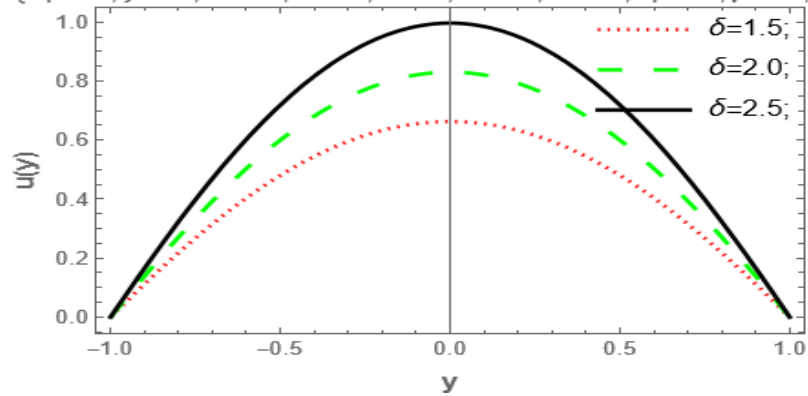


**Figure 3.4:** Effect of porous permeability on solid displacement  
 { $N_p=30; \xi=0.1; m=0.1; \kappa=0.6; G=-1; M=0.1; R=0.1; \lambda_1=0.1; \gamma=0.1; \Omega=1; \}$

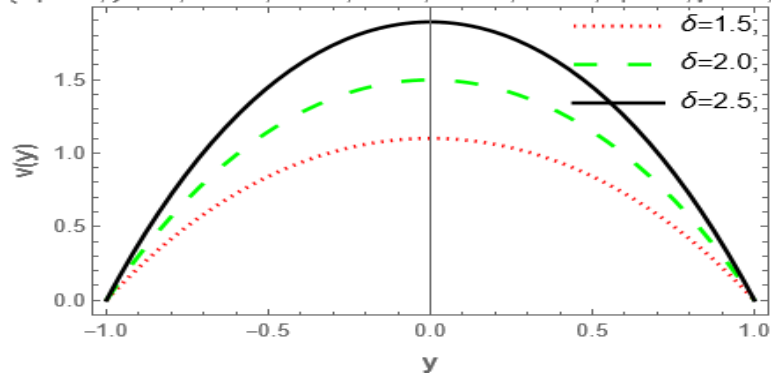


**Figure 3.5:** Porous permeability's impact on flow velocity  
 { $N_p=30; \xi=0.1; m=0.1; \kappa=0.6; G=-1; M=0.1; R=0.1; \lambda_1=0.1; \gamma=0.1; \Omega=1; \}$

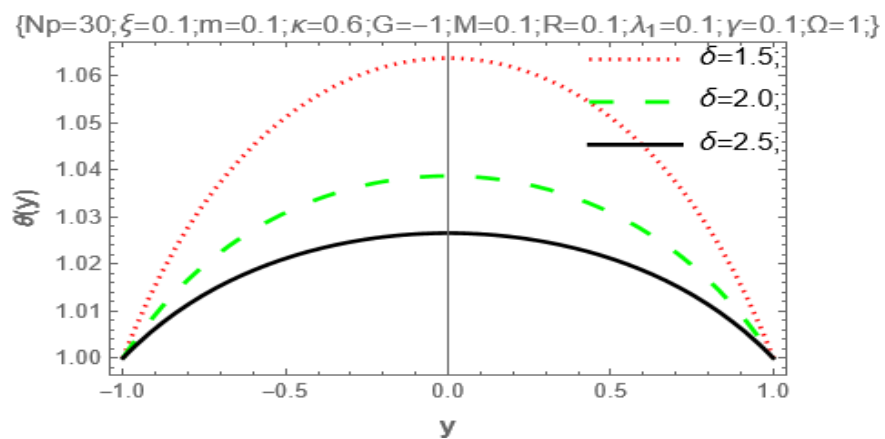


**Figure 3.6:** Effect of porous permeability on fluid temperature  
 The effect of porous permeability on the solid displacement, flow velocity and fluid temperature as shown in figures (3.4) – (3.6). The graph shows that as the porous permeability increases solid displacement and flow velocity increases but fluid temperature decreases.

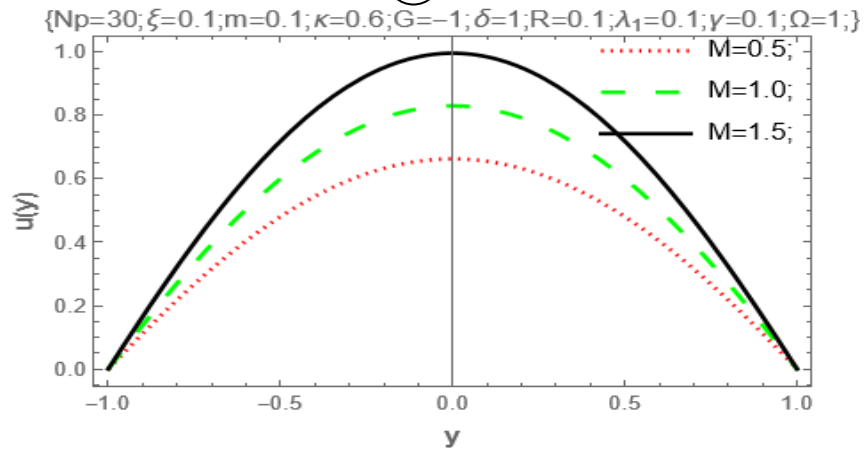


**Figure 3.7:** Effect of magnetic body force parameter on solid displacement

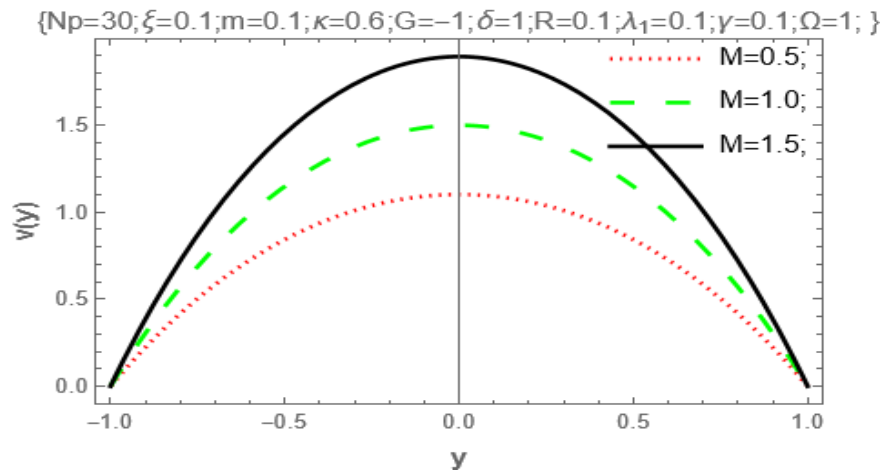


**Figure 3.8:** Effect of magnetic body force parameter on flow velocity  
 $\{Np=30; \xi=0.1; m=0.1; \kappa=0.6; G=-1; \delta=1; R=0.1; \lambda_1=0.1; \gamma=0.1; \Omega=1;\}$

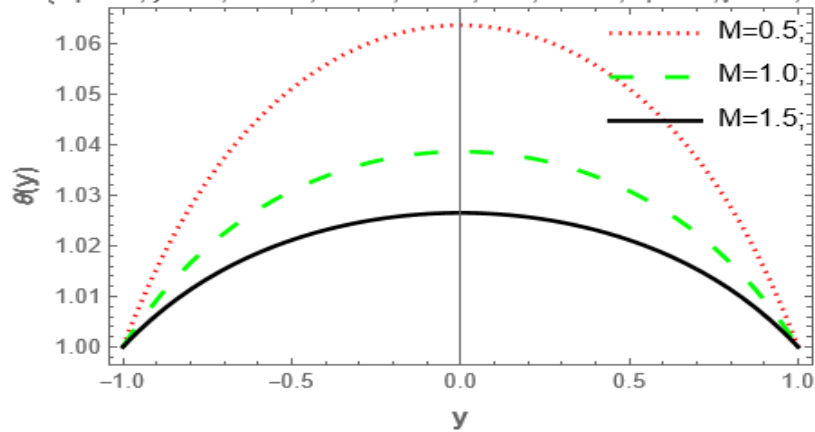


**Figure 3.9:** Effect of magnetic body force parameter on fluid temperature

The effect of magnetic body force parameter on solid displacement, flow velocity and fluid temperature as seen in figures (3.7) – (3.9). The graph shows that as the magnetic body force parameter increases the solid displacement and flow velocity while the fluid temperature decreases with increase in M.

$\{Np=30; \xi=0.1; m=0.1; \kappa=0.6; G=-1; \delta=1; M=0.1; \lambda_1=0.1; \gamma=0.1; \Omega=1;\}$

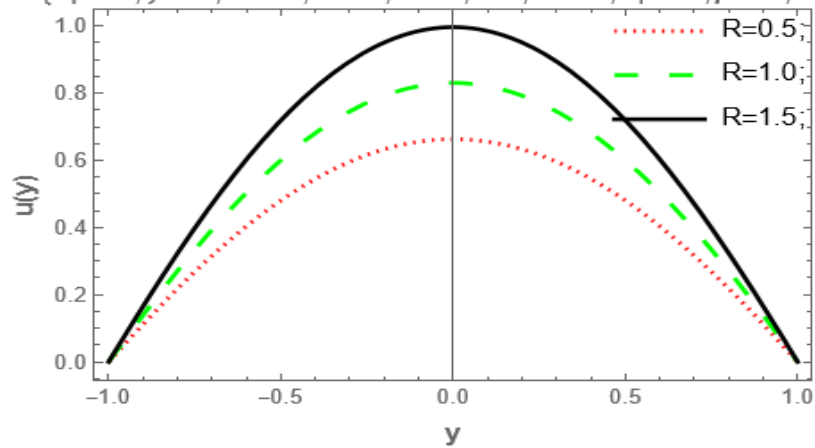




**Figure 3.10:** Effect of thermal radiation on solid displacement  
 { $Np=30; \xi=0.1; m=0.1; \kappa=0.6; G=-1; \delta=1; M=0.1; \lambda_1=0.1; \gamma=0.1; \Omega=1; \}$

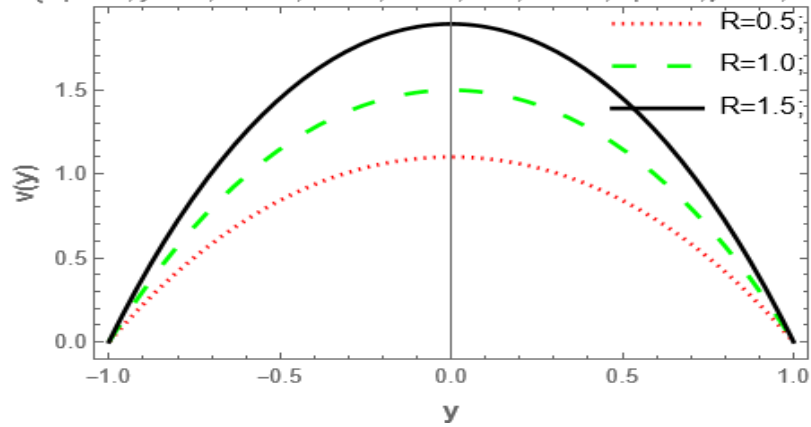


**Figure 3.11:** Effect of thermal radiation on flow velocity  
 { $Np=30; \xi=0.1; m=0.1; \kappa=0.6; G=-1; \delta=1; M=0.1; \lambda_1=0.1; \gamma=0.1; \Omega=1; \}$

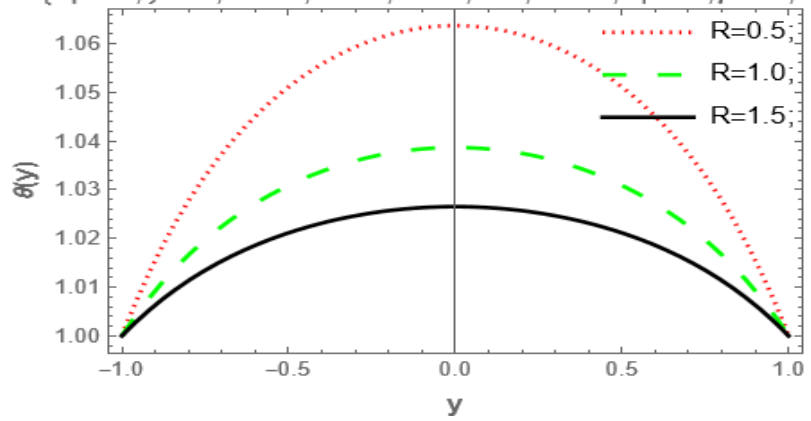




**Figure 3.12:** Effect of thermal radiation on fluid temperature  
 The effect of thermal radiation is presented on solid displacement, flow velocity and fluid temperature as seen in figures (3.10) to (3.12). The result shows that as thermal radiation increases solid displacement as well as flow velocity increases while fluid temperature decreases.

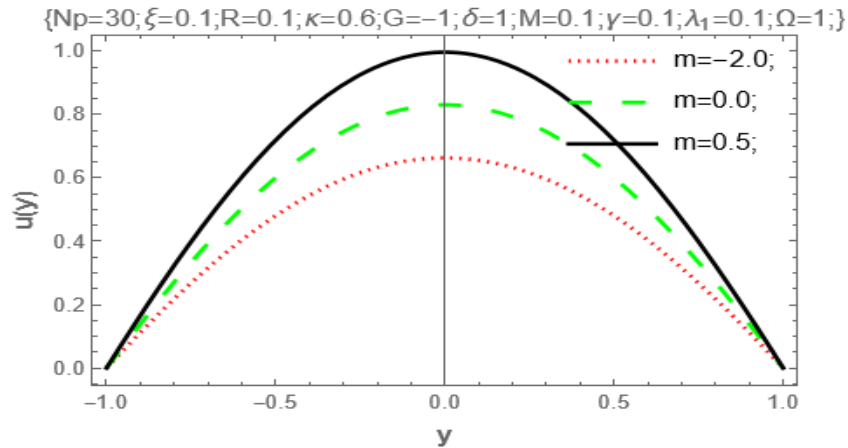


**Figure 3.13:** Effect of kinetic parameter on solid displacement  
 { $N_p=30; \xi=0.1; R=0.1; \kappa=0.6; G=-1; \delta=1; M=0.1; \gamma=0.1; \lambda_1=0.1; \Omega=1;$ }

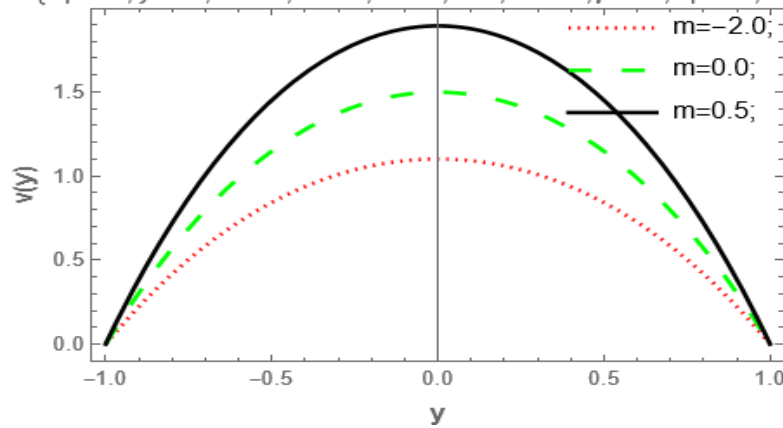


**Figure 3.14:** Effect of kinetic parameter on flow velocity

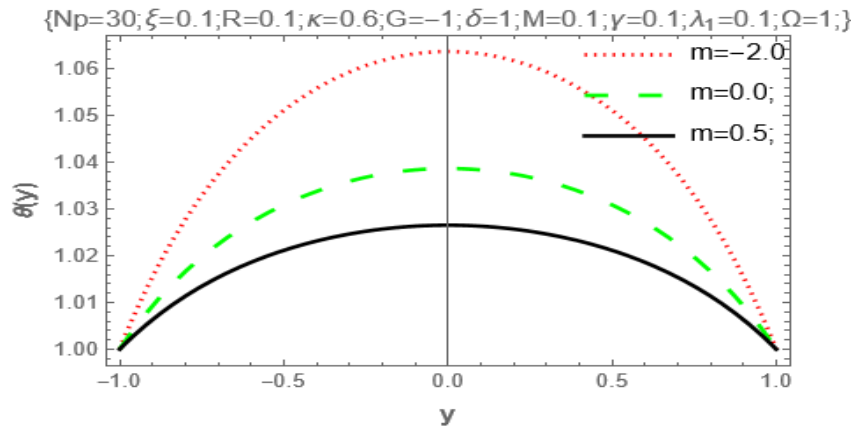


**Figure 3.15:** Effect of kinetic parameter on fluid temperature

The effect of kinetic parameter on solid displacement, flow velocity and fluid temperature is presented in figures (3.13) to (3.15). The result reveals that as thermal radiation parameter increases solid displacement and flow velocity increases as well while fluid temperature decreases.

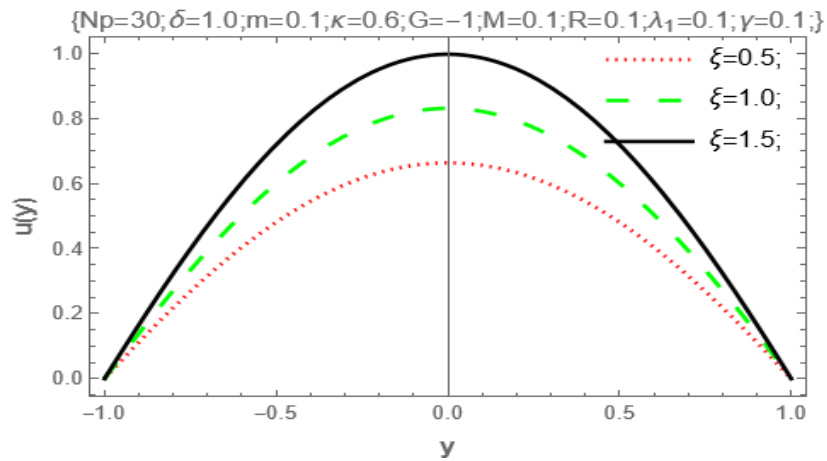


**Figure 3.16:** Effect of heat transfer coefficient on solid displacement  
 $\{Np=30; \delta=1; m=0.1; \kappa=0.6; G=-1; M=0.1; R=0.1; \lambda_1=0.1; \gamma=0.1; \}$

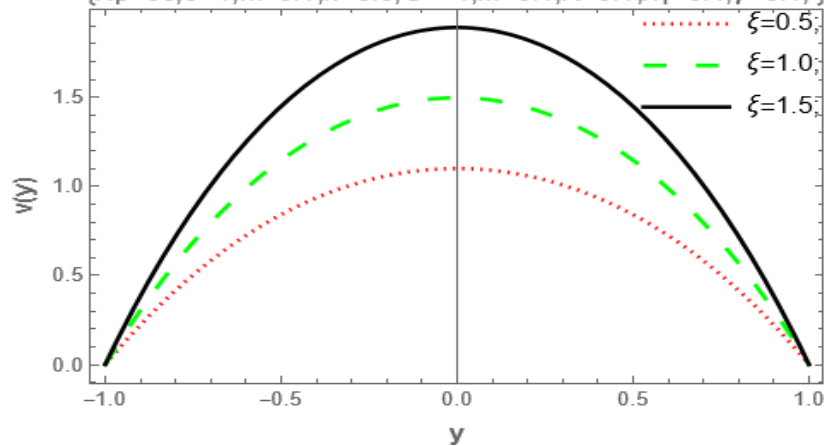


**Figure 3.17:** Effect of heat transfer coefficient on flow velocity  
 $\{Np=30; \delta=1; m=0.1; \kappa=0.6; G=-1; M=0.1; R=0.1; \lambda_1=0.1; \gamma=0.1; \}$

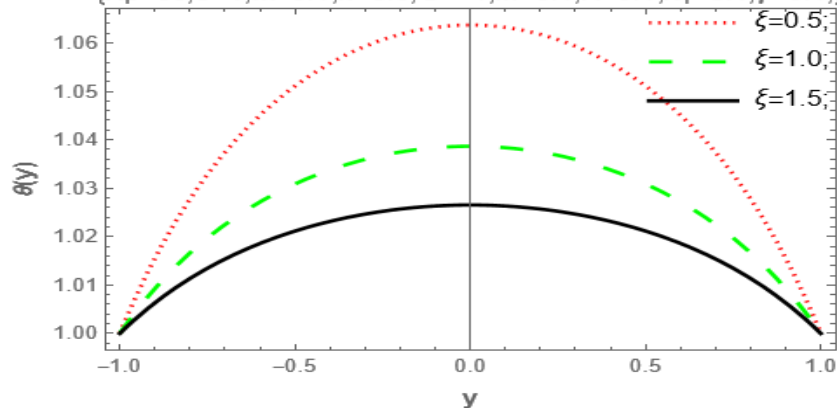


**Figure 3.18:** Effect of heat transfer coefficient on fluid temperature  
 The effect of heat transfer coefficient on solid displacement, flow velocity and fluid temperature as shown in figures (3.16) – (3.18). The result shows that an increase in heat transfer coefficient leads to an increase in solid displacement and flow velocity while an increase in heat transfer leads to a decrease in fluid temperature.

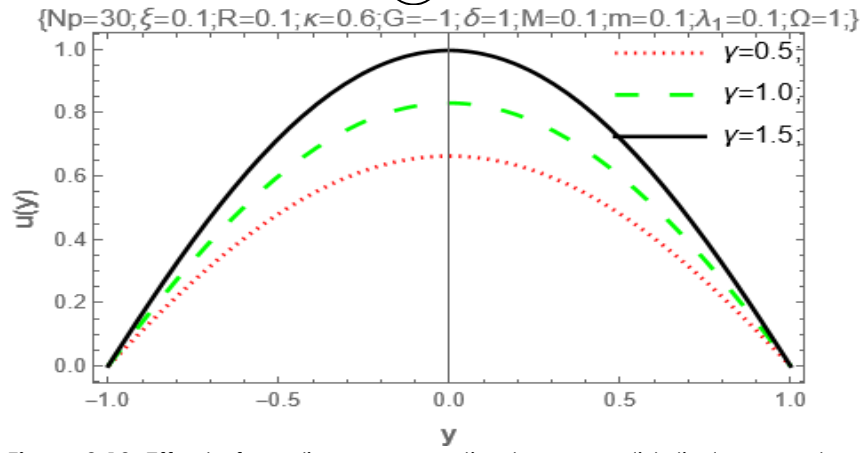


**Figure 3.19:** Effect of non-linear convective term on solid displacement  
 { $N_p=30; \xi=0.1; R=0.1; \kappa=0.6; G=-1; \delta=1; M=0.1; m=0.1; \lambda_1=0.1; \Omega=1;$ }

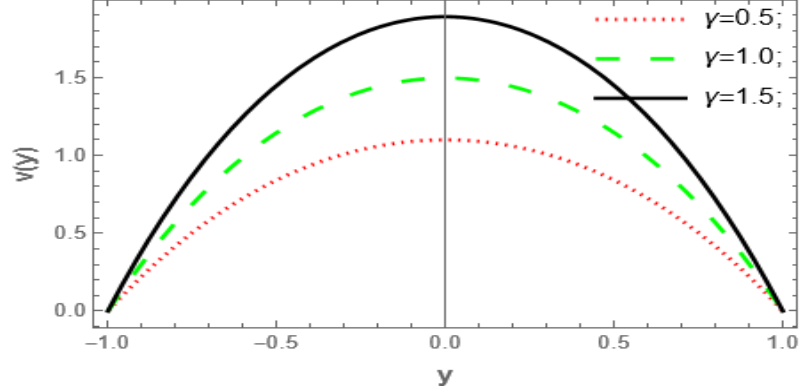


**Figure 3.20:** Effect of non-linear convective term on flow velocity  
 { $N_p=30; \xi=0.1; R=0.1; \kappa=0.6; G=-1; \delta=1; M=0.1; m=0.1; \lambda_1=0.1; \Omega=1;$ }

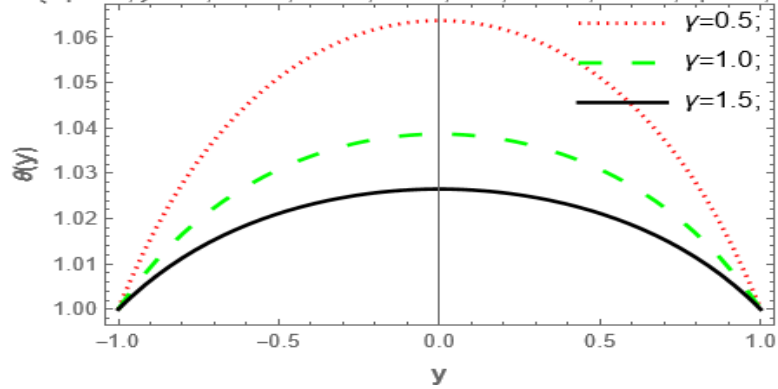




**Figure 3.21:** Effect of non-linear convective term on fluid temperature  
The effect of non-linear convective term parameter on solid displacement, flow velocity and fluid temperature as shown in (3.19) – (3.21). The graph shows that as the non-linear convective term parameter increases the solid displacement and flow velocity increases as well, while the fluid temperature decreases with increase in non-linear convective term parameter.

### **Conclusion**

This work presents a comprehensive mathematical and numerical investigation inspired by the development of a multiphysical model for transport in deformable, magneto-biothermal systems. The study focuses on magnetohydrodynamic flow and heat transfer within an electro-conductive viscoelastic flow in a vertical channel with a porous-elastic medium. The analysis incorporates thermal buoyancy and radiative flux effects, aiming to provide robust solutions for fluid velocity, solid displacement, and temperature distribution through the numerical solution of the non-dimensionalized boundary value problem.

The accuracy of computations using the Spectral Collocation Method (SCCM) and the Shooting RK-4 method is verified by comparing results with an alternative numerical approach, the Sequential Quadratic Linearization Method (SQLM). The validity of the obtained answers is confirmed through contrast with Runge-Kutta shooting quadrature and the Spectral Collocation Method (SCM). Graphical representations are utilized to illustrate the influence of parameters such as Jeffrey's viscoelasticity, viscous drag, magnetic field, radiation, and buoyancy on temperature, solid displacement, and flow velocity. These simulations have direct relevance to innovative techniques in bio-magnetic high-temperature therapy, where thermal effects are induced in the solid/fluid composite biomaterials of the human body through magnetic fields. Considering the non-Newtonian properties of interstitial fluids and their electrical conductivity resulting from the ionic nature of biofluids, an accurate representation requires a rheological model incorporating magnetic body force terms. The graphical representations highlight the impact of various physical parameters on fluid velocity, solid displacement, temperature, shear stress, and Nusselt numbers.



---

## 5.2 Recommendations

Based on the findings from this work the researcher's hereby recommend the following:

1. Utilize more method to ensure robustness and reliability in establishing the existence and uniqueness of solution
2. Compare the outcomes obtained from both methods to ensure consistency and reliability
3. Conduct sensitivity analyses to assess the robustness of the solutions with respect to variations in parameters and boundary conditions.
4. Implement Spectral numerical methods such as spectral collocation or shooting RK4 methods known for their accuracy and efficiency
5. Conduct convergences studies to ensure the numerical framework accurately captures the effects or internal heat generation across spatial and temporal resolutions
6. Conduct parametric studies to explore the interplay between nonlinear radiation, buoyancy and other relevant parameters.
7. Interpret the findings in the context of practical applications, highlighting any emergent behaviors or unexpected phenomena resulting from the combined effects
8. Explore the implications of the findings for specific applications, such as thermal management systems or electrothermal devices
9. Investigate potential coupling effects between thermal and electrical properties, considering their mutual influence on the overall system dynamics.

## References

- Abel, M., and Mashasha, A. (2007). Pairs of topology algebras. Rocky mountain journal of Mathematics, 37(1).
- Adesanya S. O., Falade, J. A., Srinivas, J., and Beg, O. A. (2017). Irreversibility Analysis for Reactive Third-Grade Fluid Flow and Heat Transfer With Convective Wall Cooling. Alexandria Eng. J., 56(1), pp. 153-160
- Ajibade, A. O. Jha, B. K.. and Omame, A. (2011). Entropy generation under the effect of suction/injection. Applied Mathematical Modelling, 35(9), 4630-4646. <https://doi.org/10.1016/j.apm.2011.03.027>
- Al-Nimr and Haddad, M. (1999). MHD free convection flow in open-ended vertical porous channels. Chemical Engineering Science, 54(12), 1883-1889.



Bear, J. (1972). *Dynamics of Fluids in Porous Media*. American Elsevier Publishing Company

Beg, O. A., Rashidi, M. M., Kavyani, N., and Islam, M. N., (2013). Entropy generation in hydromagnetic convective Von Karman swirling flow, homotopy analysis, *Int., J. Applied Math. Mech.*, 9(4) 37 -65.

Bhattacharyya, S., Kumar, V., & Singh, R. (2019). Magnetohydrodynamic flow in a porous medium. *Journal of Fluid Mechanics*, 886, 241-263.

Biot, M. A., (1941). General theory of three-dimensional consolidation, *J. Appl. Phys.*, 12(2) 155-164.

Biot, M. A., (1956). Theory of propagation of elastic waves in a fluid-saturated porous. *Journal of the Acoustical Society of America*, 28(2), 168-178.

Bowen, R. M. (1980). Incompressible porous media models by use of the theory of mixtures. *International Journal of Engineering Science*, 18(9), 1129-1148.

Bui, Ha H. Giang D. Nguyen, (2017). A coupled fluid-solid SPH approach to modelling flow through deformable porous media, *International Journal of Solids and Structures* 125, 244–264

Cess, R. D. and Sparrow, E. M. (1962). Magnetohydrodynamics flow and heat transfer about a rotating disk. *Journal of applied mechanics*, 29(1), 181-187.

Chandrasekhar, S. (1961). *Hydrodynamic and Hydromagnetic Stability*.

Cheng, A. F. (1978). Unsteady hydrodynamics of spherical gravitational collapse. *The Astrophysical Journal*, 221, 320.

Coussy, O. (1995). *Mechanics of Porous Continua*. Wiley.

Fang, T. (2013). Flow of Jeffrey fluid through a porous channel. *Journal of Non-Newtonian Fluid Mechanics*, 193, 64-71.

Finlayson, B. A. (1972). Convective instability of a magnetic fluid. *Journal of Fluid Mechanics*, 55(3), 577-590. doi: 10.1017/S0022112072000446



---

Jamalabadi, M. Y. A., Hooshmand, P., Hesabi, A., Kwak, M. K.,  
Pirzadeh, I., Keikha, A.

J., and Negahdari, M. (2016). Numerical investigation of thermal radiation and viscous effects on entropy generation in forced convection blood flow over an axisymmetric stretching sheet, *Entropy*, 18(6) 203.

Jha, B., Jha, R., Kumari Jha, D., and Jha, S. (1990). Synthesis visible absorption, photosensitization and antimicrobial activity of some butadienochromophoric chain-substituted asymmetric cyanines. *Dyes and Pigments*, 13(2), 135-154.

Kaloni, P. N., & Lou, J. (2000). Magnetic fluid effects on convective flows. *Journal of Magnetism and Magnetic Materials*, 209(1-3), 86-92. doi:10.1016/S0304-8853(99)00634-4

Khan, N. S., Shah, Z., Islam, S., Khan, I., Alkanhal, T. A., Tlili, I., (2019). Entropy generation in MHD mixed convection non-Newtonian second-grade nanoliquid thin film flow through a porous medium with chemical reaction and stratification, *Entropy*, 21(2) 139. 35

Kumar, M., Reddy, G. J., RaviKiran, G., Aslam, M. A. M., and Anwar Beg, O., (2019): Computation of entropy generation in dissipative transient natural convective viscoelastic flowm *Heat Transfer Asian Research*, 1-26, DOI: 10.1002 htj. 21421.

Magyari, E., and Pantokratoras, A. (2011). Aiding and opposing mixed convection flows over the Riga-plate. *Communications in nonlinear science and numerical simulation*, 16(8), 3158-3167.

Mansour, M. (1990). Variability analysis of timber bridge responses. *Structural safety*, 9(1), 41-58.

Mallikarjuna, B., Srinivas, J., Gopi Krishna, G., Anwar Beg, O., and Kadir, A., (2021). Spectral Numerical study of Entropy Generation in Magneto-Convective Viscoelastic Biofluid flow through poro-elastic media with thermal radiation and buoyancy effects

Makinde, O., and Moitsheki, R. (2007). Some invariant solutions for a microwave heating model. *Applied Mathematics and Computation*, 191(2), 308-313.

Makinde, O. D., and Ibrahim, W. (2011): Double –diffusive in mixed convection and MHD



stagnation point flow of nanofluid over a stretching sheet. *Journal of nanofluids*, 4(1), 28-37.

Manzoor, N., Magbool, K., Anwar Beg, O., and Shaheen, S., (2018). Adomain decomposition solution for propulsion of dissipative magnetic Jeffrey Biofluid in a ciliated channel containing a porous medium with forced convection heat transfer, *Heat Transfer*, 1-26, DOI: 10.1002/htj. 21394.

Miyatake, K., Nakano, Y., and Kitaoka, S. (1976). Pantothenate synthetase of *Escherichia coli* B I. Physicochemical properties. *The Journal of Biochemistry*, 79(3), 673-678.  
<https://doi.org/10.1093/oxfordjournals.jbchem.a131112>

Ouyang, X., Yang, S., & Wang, X. (2020). Flow through porous media with elastic deformation. *Journal of Fluid Mechanics*, 894, A22. doi: 10.1017/jfm.2020.345

Ramana Murthy, J. V., Anwar Beg, O., Srinivas, J. Ramana Murthy, J. V., (2017). Entropy generation analysis of radiative heat transfer effects on channel flow of two immiscible couple stress fluids, *J. Brazilian Soc. Mech. Sci. Eng.*, 39 2191-2202

Ramesh, K., Tripathi, D., Anwar Beg, O., and Kadir, A., (2018). Slip and hall current effects on viscoelastic fluid particle suspension flow in a peristaltic hydromagnetic blood micropump, *Iranian J. Science Tech. Trans. Mech. Eng.* Doi.org/10.1007/s40997-018—230-5

Rohan, E., Lukes, V., & Zeman, J. (2019). Coupled approach of solid and fluid in a deformable porous medium. *Transport in Porous media*, 128(2), 531-554. doi: 10.1007/S11242-019-01253-5

Rosseland, S. (1931). Mechanische integration von differentialgleichungen. *Die naturwissenschaften*, 27(44), 729-735.

Sheikholeslami, M., & Ganji, D. D. (2015). Magnetohydrodynamic flow of a nanofluid in a porous channel. *Journal of Molecular Liquids*, 201, 102-111. doi: 10.1016/j.molliq.2014.12.048

Shojaefard, M. H., Noorpoor, A. R., Bozchaloe, D. A., and Ghaffarpour, M. (2005). Transient thermal analysis of engine exhaust valve. *Numerical heat transfer, part A: Applications*, 48(7), 627-644.

Sochi, T. (2010). Non-Newtonian fluid mechanics. *Journal of Non-Newtonian Fluid Mechanics*, 165(11-12), 573-584.



Shukla, N., Rana, P., Anwar Beg, O., Kadir, A., and Singh, B. (2018). Unsteady electromagnetic radiative nanofluid stagnation-point flow from a stretching sheet with chemically reactive nanoparticles, Stefan blowing effect and entropy generation, *Proc. I Mech E; Part N-J Nanomaterials, Nanoeng, Nanosystems*. DOI: 10.1177/2397791418782030.

Siddiqa, S., & Hossain, M. A. (2013). Effects of magnetic field on convective flow of a nanofluid. *International Journal of Thermal Sciences*, 64, 162-172. doi: 10.1016/j.ijthermalsci.2012.09.004

Siegel, R., & Howell, J. R. (1972). *Thermal Radiation Heat Transfer*. McGraw-Hill.

Takhar, H. S., & Singh, A. K. (1998). Radiation effects on MHD free convection flow. *International Journal of Thermal Sciences*, 37(5), 412-420.

Tanner (1968). Non-Newtonian fluids. *Journal of Applied Mechanics*, 35(2), 267-274.

Varjavelu, K., Siva Reddy, P., & Chamkha, A. J. (2011). Radiation effects on unsteady MHD free convection flow past a vertical plate. *International Journal of Thermal Sciences*, 50(5), 674-683. doi: 10.1016/j.ijthermalsci.2010.12.013

Viskanta, R. (1966). Heat transfer by conduction and radiation in absorbing and scattering media. *Journal of Heat Transfer*, 88(2), 143-150.

Zhao, W.-J., Wang, J., Qi, Z.-Y., & Liu, H.-Q. (2023). Study of deep transportation and plugging performance of deformable gel particles in porous media, *Petroleum Science*